Title

Energetics of Semienclosed Basins with Two-Layer Flows at the Strait

Journal

Journal of Physical Oceanography, 44(3)

ISSN

0022-3670

Authors

Cessi, Paola
Pinardi, Nadia
Lyubartsev, Vladislav

Publication Date

2014-03-01

DOI

10.1175/jpo-d-13-0129.1

Peer reviewed

Energetics of Semienclosed Basins with Two-Layer Flows at the Strait

PAOLA CESSI

Scripps Institution of Oceanography, University of California, San Diego, La Jolla, California

NADIA PINARDI

Department of Physics and Astronomy, University of Bologna, Italy

VLADISLAV LYUBARTSEV

Centro Euro-Mediterraneo sui Cambiamenti Climatici, Bologna, Italy

(Manuscript received 12 June 2013, in final form 26 November 2013)

ABSTRACT

Examination of the energy budget for semienclosed seas with two-layer exchange flow at the strait shows that the energy flux at the open portion of the boundary (the strait) is proportional to the surface buoyancy flux integrated over the basin area, with the constant of proportionality given by the interface depth. When the surface buoyancy flux is positive, the energy flux is negative: these types of basins have an estuarine circulation. Antiestuarine basins have a negative surface buoyancy flux, which provides a positive energy flux, augmenting the wind work in powering the circulation. The energy budget for the semienclosed seas with vertically separated flows at the strait is examined using reanalysis products for four major semienclosed basins: the Mediterranean and Red Seas (antiestuarine) and the Black and Baltic Seas (estuarine). Important differences in the relative contribution to the energy budget of the wind work versus the surface buoyancy flux are found within basins of the same type, and these differences help explain some qualitative aspects of the basins' flow.

1. Introduction

Semienclosed or adjacent seas are limited areas of the World Ocean connected to another sea or ocean by one or more outlets that are shallower than the maximum depth of the enclosed basin. Pickard and Emery (1982) (cf. their 172–174 and our Fig. 1) differentiate between the semienclosed seas with horizontally and vertically separated inflow and outflow regimes at the strait. In this study we consider only semienclosed seas with a single outlet and strait flows that are separated vertically: in this category a fundamental distinction occurs between basins with an estuarine or an antiestuarine circulation. The flow at narrow and shallow straits is often approximated with two layers, and the estuarine case is characterized by a seaward freshwater outflow in the top layer and an inflow of saltier water below. The antiestuarine case has a reversed flow at the strait (Fig. 1). There are four major semienclosed seas with two-layer flows at the strait in the World Ocean: the Mediterranean, Red, Baltic, and Black Seas. The first two are antiestuarine and the last two are estuarine.

Classically, the Knudsen relations (Knudsen 1900) are used to explain the qualitative distinction between the estuarine and antiestuarine vertical circulation at the strait. The relations derive simply from mass and salinity budgets within the semienclosed basin, with no reference to the wind forcing. While it is possible to obtain circulations in semienclosed seas driven only by negative surface buoyancy flux (Spall 2003), the wind forcing has been shown to be essential in powering the circulation at least in the Mediterranean (Korres et al. 2000) and in the Black Seas (Rachev and Stanev 1997). Indeed, Knudsen relations merely provide the sign of the circulation at the strait, with no reference to its basin average strength. To have some information about the vigor of the circulation, and about the relative importance of wind and buoyancy forcing, other diagnostics need to be examined.

A traditional approach is to consider the basin-averaged energy budgets with all forcings. Analysis of the energy

Corresponding author address: Paola Cessi, 9500 Gilman Drive, UCSD-0213, La Jolla, CA 92093-0213.
E-mail: pcessi@ucsd.edu

DOI: 10.1175/JPO-D-13-0129.1

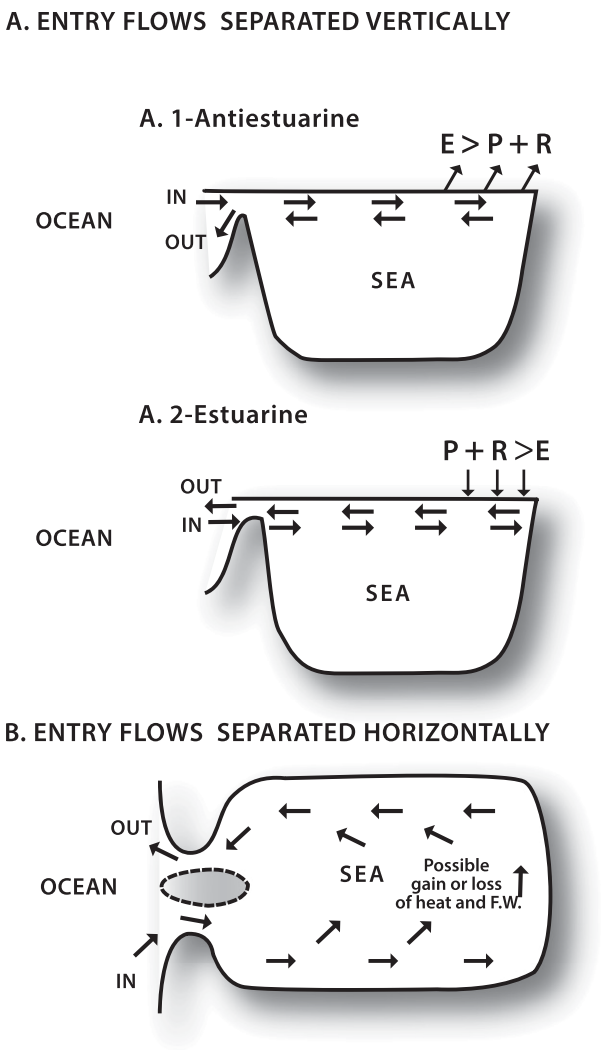

FIG. 1. The classification of semienclosed (or adjacent) seas according to Pickard and Emery (1982). Basins of type A have a single strait where the exchange flow is separated vertically: this type is further subdivided into antiestuarine, denoted by A1, and estuarine, denoted by A2. Basins of type B have multiple straits with substantial net flow into or out of each strait. [Reproduced with modifications from Pickard and Emery (1982).]

budgets of the ocean is one of the several ways to gain insight into the processes that control the circulation, its strength, and characteristics. The global energy budget has recently been revisited (Wunsch and Ferrari 2004), and the conclusion is that the mechanical forcing, through surface wind stress and tides, is what powers the oceanic motion. For the global ocean, the conversion term between kinetic energy and potential energy (or available potential energy) is bounded by a term proportional to the molecular diffusivity (Paparella and Young 2002; Winters and Young 2009) and is thus too small to account for observed levels of kinetic energy. This point of view has been questioned by a series of authors [e.g., Gayen et al. (2013) and references therein], arguing that a substantial circulation can be obtained with surface buoyancy forcing alone. However, the energetics of semienclosed basins are different from the global ocean because of the lateral open-boundary conditions and the implied import/export of energy that should balance the surface energy inputs by winds, buoyancy, and tides.

The question that we would like to address is can energy balances explain the differences between estuarine and antiestuarine basins and among the same kind of semienclosed seas, for example, the Mediterranean and Red Seas or the Baltic and Black Seas?

The key difference between the closed, global ocean and semienclosed sea energetics comes from the open portion of the boundary, where a flux of energy and a flux of buoyancy can be exchanged with the adjacent ocean. For the global ocean, over long time scales, the net surface buoyancy flux integrates to zero or else a statistical steady state could not be reached.[1] When considering subsections of the global ocean, in particular semienclosed seas, the net surface buoyancy flux may not vanish, because it can be balanced by a buoyancy flux through the strait. In turn, the buoyancy flux through the strait has important consequences on the flow in the basin, in addition to the wind work.

The buoyancy flux through the strait is associated with a flux of energy (kinetic plus potential plus pressure work), so there is a relation between the energy and buoyancy fluxes. In this study, we show how these two fluxes can be related for enclosed seas with one outlet and with vertically separated entry flows. Specifically, it will be shown that, in the limit of a small Froude number when the kinetic energy is much smaller than the potential energy, the energy (potential plus pressure work) flux at the strait and the surface buoyancy flux are linearly proportional to each other, with the constant of proportionality given by the height of the interface between the two layers at the strait. The validity of the relation is verified for the case of the Mediterranean Sea, where the energy flux at the open boundary, the height of the interface at the strait, and the surface heat and freshwater fluxes can all be evaluated independently from a model reanalysis dataset.

The energy balance thus obtained can be used to contrast the estuarine with the antiestuarine character of the circulation in different semienclosed seas and among

[1] In a changing climate there might be a long-term trend in the oceanic temperature, but this term is small compared to the energy sources and sinks.

different basins with the same estuarine or antiestuarine character. In particular, the energetics illustrate that, while the wind work always represents a source of energy in the time-averaged budget, the surface heat and freshwater fluxes, mediated by the energy flux at the open boundary, can be a source (antiestuarine case) or a sink (estuarine case) of energy, which is, in general, comparable in magnitude to the mechanical power.

The paper is organized as follows: section 2 describes the energy equations, section 3 finds the relationship between the lateral energy flux and the surface buoyancy, in section 4 we apply the energetics to semienclosed seas, and section 5 offers the conclusions.

2. Conservation equations

We consider the Boussinesq hydrostatic equation where the density is referenced around the constant value ρ_o. The system is governed by

$$\frac{Du}{Dt} - fv + \frac{p_x}{\rho_o} = \nabla_h \cdot \nu \nabla_h u + (\nu_v u_z)_z + \delta(z)\frac{\tau^x}{\rho_o}, \quad (1)$$

$$\frac{Dv}{Dt} + fu + \frac{p_y}{\rho_o} = \nabla_h \cdot \nu \nabla_h v + (\nu_v v_z)_z + \delta(z)\frac{\tau^y}{\rho_o}, \quad (2)$$

$$\frac{p_z}{\rho_o} = b, \quad (3)$$

$$u_x + v_y + w_z = 0, \quad \text{and} \quad (4)$$

$$\frac{Db}{Dt} = \nabla_h \cdot \kappa \nabla_h b + (\kappa_v b_z)_z, \quad (5)$$

where x, y, and z are Cartesian orthogonal coordinates with z parallel and opposite to gravity; $(D/Dt) = \partial_t + \mathbf{u} \cdot \nabla_h + w\partial_z$; ∇_h is the horizontal gradient operator; $\mathbf{u} = (u, v)$ is the horizontal velocity field; g is the gravity; p is the pressure; ν and ν_v are the horizontal and vertical eddy viscosities, respectively; κ and κ_v are the horizontal and vertical diffusivities, respectively; $\boldsymbol{\tau} = (\tau^x, \tau^y)$ is the wind stress; f is the Coriolis parameter; and $\delta(z)$ is the delta function at $z = 0$. The buoyancy is defined as

$$b \equiv -g\frac{\rho - \rho_o}{\rho_o}, \quad (6)$$

that is, as the departure from the Boussinesq reference value ρ_o and accordingly, pressure omits the term $-\rho_o g z$ associated with the constant density.

We consider a linear equation of state (EOS),[2] such that

$$b = g(\beta_T T - \beta_S S), \quad (7)$$

where T is the temperature, S is the salinity, and β_T and β_S are the coefficients of thermal and haline expansion, respectively. With a linear EOS, the surface flux of buoyancy Q_b is given by

$$Q_b = \frac{g\beta_T}{\rho_o C_w} Q_H - \beta_S S_0 g(E - P - R), \quad (8)$$

where Q_H is the heat flux (with a sign convention such that it is positive when heat is entering the ocean), C_w is the specific heat capacity, S_0 is the surface salinity, and $E - P - R$ is the evaporation minus precipitation and runoff.[3]

Because we are concerned with semienclosed basins, we consider a section of the boundary to be open: the arclength of the open section in the horizontal plane is denoted by OB. We now derive the total energy equation, starting from the kinetic energy, obtained by multiplying the horizontal momentum equations [(1) and (2)] by $\mathbf{u}$. Integration over the volume of the domain, denoted by angle brackets, gives

$$\partial_t \frac{\langle u^2 + v^2 \rangle}{2} = \langle wb \rangle + \int_A \frac{\boldsymbol{\tau} \cdot \mathbf{u}_s}{\rho_o} dx\, dy - \int_{\mathrm{OB}} \int \left(\frac{u^2 + v^2}{2} + \frac{p}{\rho_o} \right) \mathbf{u} \cdot \hat{\mathbf{n}}\, dz\, dl - \langle \nu(|\nabla_h u|^2 + |\nabla_h v|^2) \rangle$$
$$- \langle \nu_v (u_z^2 + v_z^2) \rangle - \int_{\mathrm{OB}} \int \nu \frac{\nabla_h (u^2 + v^2)}{2} \cdot \hat{\mathbf{n}}\, dz\, dl, \quad (9)$$

where $\mathbf{u}_s$ is the surface velocity field. Notice that $\hat{\mathbf{n}}$ denotes the outward direction normal to the strait, so that $\mathbf{u} \cdot \hat{\mathbf{n}}$ is negative when the velocity at the strait is into the basin.

To eliminate the conversion term $\langle wb \rangle$, we need to form the potential energy equation, obtained by multiplying the buoyancy equation [(5)] by z and integrating over the domain. We obtain

[2] The results are extended to a nonlinear EOS in appendix A.

[3] All fluxes, Q_b, Q_H, and $E - P - R$, are per unit area.

$$\partial_t\langle zb\rangle = \langle wb\rangle - \int_{\mathrm{OB}}\int z(b\mathbf{u} - \kappa\nabla_h b)\cdot\hat{\mathbf{n}}\,dz\,dl - \langle \kappa_v b_z\rangle. \tag{10}$$

In steady state, for a closed domain, the second term on the right-hand side of (10) vanishes, and the only contribution to the conversion term $\langle wb\rangle$ is $\langle\kappa_v b_z\rangle$, which is small for small diffusivity. However, for a semienclosed domain, the second term on the right-hand side of (10) does not vanish, and, as will be shown in section 4, it can be as large as the rate of the wind work. Eliminating $\langle wb\rangle$ between (9) and (10), the mechanical energy equation is obtained, given by

$$\partial_t\left\langle\frac{u^2+v^2}{2} - zb\right\rangle = \int_A \frac{\boldsymbol{\tau}\cdot\mathbf{u}_s}{\rho_o}\,dx\,dy + F + \langle\kappa_v b_z\rangle - \langle\nu(|\nabla_h u|^2 + |\nabla_h v|^2)\rangle - \langle\nu_v(u_z^2 + v_z^2)\rangle - \int_{\mathrm{OB}}\int\left[\nu\frac{\nabla(u^2+v^2)}{2}\right]\cdot\hat{\mathbf{n}}\,dz\,dl + D, \tag{11}$$

where we have made the definitions

$$F \equiv -\int_{\mathrm{OB}}\int\left(\frac{u^2+v^2}{2} + \frac{p}{\rho_o} - zb\right)\mathbf{u}\cdot\hat{\mathbf{n}}\,dz\,dl \tag{12}$$

and

$$D \equiv -\int_{\mathrm{OB}}\int\kappa z\nabla_h b\cdot\hat{\mathbf{n}}\,dz\,dl. \tag{13}$$

The term F represents the flux of energy through the strait, and it is the combination of three terms: the flux of kinetic energy, the pressure work, and the flux of potential energy. The flux of potential energy must be considered in conjunction with the pressure work term because it is only the combination $p/\rho_o - zb$ that is independent of the arbitrary reference value of the density. The term D is the diffusive flux of potential energy at the strait.

Throughout the derivation we make the rigid lid approximation, so that $w = 0$ at the surface ($z = 0$). This implies that we neglect any net flow through the strait, and hence, in the volume-averaged Boussinesq mass balance

$$\int_{\mathrm{OB}}\int\mathbf{u}\cdot\hat{\mathbf{n}}\,dz\,dl = \int_A (P + R - E)\,dx\,dy \tag{14}$$

we neglect the right-hand side contribution. Thus, in this formulation the freshwater flux appears as a salinity flux in the buoyancy budget and does not appear in the mass balance. The rigid lid assumption leads to slightly modified "Knudsen relations," as explained in appendix B.

We also write the buoyancy equation integrated over the domain; that is,

$$\partial_t\langle b\rangle + \int_{\mathrm{OB}}\int(b\mathbf{u} - \kappa\nabla_h b)\cdot\hat{\mathbf{n}}\,dz\,dl = \int_A Q_b\,dx\,dy, \tag{15}$$

where Q_b is the buoyancy flux at the surface given in (8).

3. Estimating the energy flux through the strait

In this section, we argue that it is possible to relate the flux of energy through the strait (12) to the buoyancy flux into the basin on the right-hand side of (15). This relation is obtained after making the following approximations:

1) The equation of state is linearized as in (6) at the strait only (cf. appendix A). This approximation requires the strait to be shallow.
2) The velocity at the strait is dominated by the along-strait component. This approximation requires the strait to be narrow.
3) The flow is approximately in two layers.
4) The barotropic (depth independent) velocity at the strait is negligible relative to the baroclinic component, so we approximate the right-hand side of (14) with zero.

Two-layer system

We evaluate F for a two-layer system, with upper-layer buoyancy b_1 and lower-layer buoyancy b_2, both constant. We assume that the pressure is in hydrostatic balance, so that

$$\frac{p_1}{\rho_o} = b_1 z + \frac{p_o(x,y,t)}{\rho_o} \quad \text{and}$$
$$\frac{p_2}{\rho_o} = b_2 z + \frac{p_o(x,y,t)}{\rho_o} - (b_1 - b_2)\,h_1(x,y,t), \tag{16}$$

where h_1 is the thickness of the upper layer or, equivalently, the depth of the interface between the two layers, and p_o is the pressure at the rigid lid. The thickness of the lower layer is denoted by h_2, and the total depth of the

strait is $h = h_1 + h_2$. We note that the term $zb - p$ for a two-layer system is given by

$$zb_1 - \frac{p_1}{\rho_o} = -\frac{p_o}{\rho_o} \quad \text{and} \tag{17}$$

$$zb_2 - \frac{p_2}{\rho_o} = -\frac{p_o}{\rho_o} + (b_1 - b_2)h_1 . \tag{18}$$

From (17) and (18), it is clear that the energy flux arises from the combination of the potential energy flux and the pressure work, and these two terms are of the same order.

Assuming that the velocity along the strait u is much larger than the velocity v and that u, h_1, and p_o are all constant across the strait, the integrals in (12) can be explicitly carried out and we get

$$F = l\left[\frac{h_1 u_1^3 + h_2 u_2^3}{2} - (b_1 - b_2)h_1 h_2 u_2\right], \tag{19}$$

where l denotes the width of the strait,[4] and u_1 and u_2 are the upper- and lower-layer velocities at the strait, respectively (positive into the semienclosed sea). The mass conservation constraint (14) for the two-layer system is

$$u_1 h_1 = -u_2 h_2 \tag{20}$$

and (20) has been used to eliminate terms proportional to p_o. We can further rewrite (19) by using (20), as

$$F = -l h_1 u_1 \Delta E, \quad \text{where} \tag{21}$$

$$\Delta E \equiv \frac{u_2^2 - u_1^2}{2} - (b_1 - b_2)h_1 \tag{22}$$

is the mechanical energy per unit mass entering at the strait. Thus, F represents the flux through the strait of mechanical energy due to the flux of kinetic and potential energy plus the work done by the pressure. We note that the quantity defined in (22) is the internal Bernoulli function (per unit mass) introduced by Pratt and Whitehead (2008).

Alternatively, we can recast (19) in terms of the composite Froude number G, defined as

$$G^2 \equiv (b_1 - b_2)^{-1}\left(\frac{u_1^2}{h_1} + \frac{u_2^2}{h_2}\right). \tag{23}$$

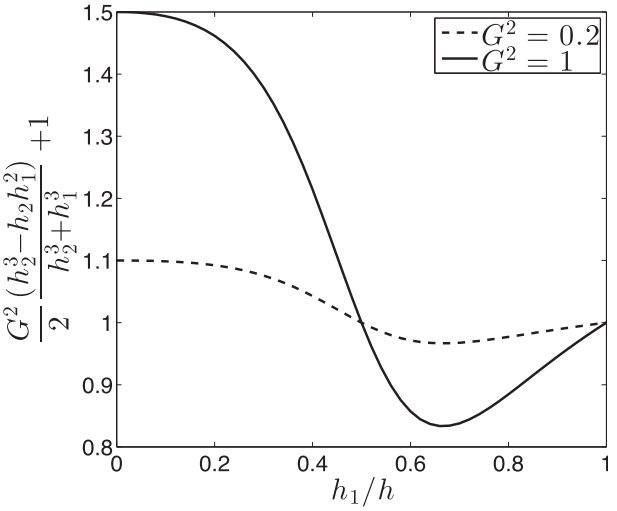

FIG. 2. The quantity $\{(G^2/2)[(h_2^3 - h_1h_1^2 - h_1^3)/(h_2^3 + h_1^3)] + 1\}$ as a function of the ratio h_1/h, where $h = h_1 + h_2$ for two values of the composite Froude number G. For small G, this quantity stays close to 1.

Then F becomes

$$F = l h_1^2 u_1 (b_1 - b_2)\left[\frac{G^2}{2}\frac{(h_2^3 - h_2 h_1^2)}{h_2^3 + h_1^3} + 1\right], \tag{24}$$

and D is given by[5]

$$D = l(b_1 - b_2)h_1 \kappa \nabla_h h_1 \cdot \hat{\mathbf{n}}. \tag{25}$$

The advantage of the expressions in (24) and (25) is that they easily relate F and D to the buoyancy flux through the strait, which is given in the two-layer case by

$$\int_{\mathrm{OB}} \int b\mathbf{u} \cdot \hat{\mathbf{n}}\, dz\, dl = -l(b_1 - b_2)h_1 u_1 . \tag{26}$$

In (26) all the quantities are evaluated at the strait. Using (15) to relate the buoyancy flux at the open boundary to the surface buoyancy flux and eliminating u_1 between (24) and (26), we finally arrive at the relation

$$F = -h_1\left(\int_A Q_b\, dx\, dy - \partial_t \langle b \rangle - \frac{D}{h_1}\right)\left[\frac{G^2}{2}\frac{h_2(h_2^2 - h_1^2)}{h_2^3 + h_1^3} + 1\right], \tag{27}$$

which relates the energy flux through the strait, $F + D$, to the buoyancy flux Q_b integrated over the semienclosed basin. Figure 2 shows the quantity inside the square

[4] For simplicity, in this subsection, we take the depth of the strait h to be constant, but the derivation can be carried through without this assumption.

[5] To evaluate the diffusive term in the two-layer model, we set $b = b_1\mathcal{H}(z + h_1) + b_2[1 - \mathcal{H}(z + h_1)]$, where $\mathcal{H}$ is the Heaviside function, with b_1 and b_2 constant and h_1 a function of space and time.

brackets on the rhs of (27) as a function of h_1/h, illustrating that it is close to unity when G^2 is small. Therefore, the approximation

$$F + D \approx -h_1 \left(\int_A Q_b \, dx \, dy - \partial_t \langle b \rangle \right) \tag{28}$$

is excellent in the limit of small Froude number. Observed Froude numbers for the Mediterranean side of the Strait of Gibraltar are estimated to be about $G^2 = 0.2$ (Sannino et al. 2002), with similar values in the Bosphorus Strait (Gregg and Özsoy 1999) and Bab el Mandab (Murray and Johns 1997). Thus, for a two-layer exchange flow at a small Froude number, there is a direct relation between the energy flux at the strait and the net surface buoyancy flux, with a constant of proportionality approximately given by the depth of the layer interface.

We note that to arrive at (28), it is very important to neglect the barotropic component of the flow at the strait, otherwise an additional term contributes to F, which is proportional to the correlation of the barotropic flow with the vertically averaged pressure. Such a term cannot obviously be related to the buoyancy budget or other global constraints. While this term is clearly negligible in exchange flows of basins with a single strait (type A in Fig. 1), it is likely an important contribution in semienclosed seas with multiple strait connections to the ocean (type B in Fig. 1).

Finally, we can rewrite the mechanical energy equation as

$$\partial_t \left\langle \frac{u^2 + v^2}{2} \right\rangle - \langle (z + h_1) b_t \rangle \approx -h_1 \int_A Q_b \, dx \, dy + \int_A \frac{\boldsymbol{\tau} \cdot \mathbf{u}_s}{\rho_o} dx \, dy + \langle \kappa_v b_z \rangle - \langle \nu (|\nabla u|^2 + |\nabla v|^2) \rangle$$
$$- \langle \nu_v (u_z^2 + v_z^2) \rangle - \int_{\mathrm{OB}} \int \nu \frac{\nabla (u^2 + v^2)}{2} \cdot \hat{\mathbf{n}} \, dz \, dl. \tag{29}$$

With the approximation (28), the flux of energy through the boundary is explicitly related to the surface flux of buoyancy, making it clear that in order for the buoyancy flux to be a source of energy, Q_b needs to be negative. This is reasonable since adding buoyancy at the surface (heating or freshening at the top) decreases the (potential) energy of the system. Another interpretation is to note that an open-boundary input of energy ($F > 0$) requires $u_1 > 0$ and $u_2 < 0$ [cf. (21)]. Because the outward flow at the strait occurs at a lower buoyancy, in the interior of the basin a convective-type circulation must occur whereby light water is transformed into denser water, in accordance with the loss of buoyancy described by (28) when $Q_b < 0$. Whether this overturning circulation occupies a shallow region of the basin, or involves a deep cell, depends on the overall level of energy given by (29), and this depends on the rate of the wind work as well. When $Q_b > 0$, both F and u_1 are negative, so that buoyant water is flowing out and dense water is flowing in at the strait. Without wind forcing this exchange at the strait implies an interior diffusive circulation, that is, a sluggish flow in the limit of small diffusivity.

In (9) and (29), we have not included the work done by the tides because the reanalyses that we consider in section 4 do not include this forcing term. Here, we note that, for the Mediterranean, the flux of tidal energy at the Strait of Gibraltar has been estimated to be $1.6 \times 10^{-10}\,\mathrm{m^2\,s^{-3}}$ (Tsimplis et al. 1995), that is, approximately one order of magnitude smaller than the rate of the wind work.

In the following, we give estimates only of F and the rate of the wind work from numerical models' output, while we do not have a way to evaluate the remaining diffusive and viscous terms. However, we note that the term $\langle \kappa_v b_z \rangle$ can be calculated from the rate of turbulent kinetic energy dissipation ε using the Osborn relation (Osborn 1980)

$$\kappa_v b_z = \Gamma \varepsilon, \tag{30}$$

with $\Gamma = 0.2$, a dimensionless efficiency constant.

For the Mediterranean Sea, Cuypers et al. (2012) measured an average $\varepsilon = 1.5 \times 10^{-9}\,\mathrm{m^2\,s^{-3}}$ along a trans-Mediterranean track, giving an estimate of $\langle \kappa_v b_z \rangle = 3 \times 10^{-10}\,\mathrm{m^2\,s^{-3}}$, which, as shown in the next section, is about a factor of 4 smaller than F.

4. Semienclosed seas with vertically separated flows at the strait

Of the semienclosed seas with two-layer exchange at the strait, we examine the four major ones: the Mediterranean and Red Seas (antiestuarine) and the Black and Baltic Seas (estuarine).

First, we analyze the Mediterranean Sea, where a comprehensive high-resolution reanalysis is available that allows us to calculate F, Q_b, and $\langle b_t \rangle$ and thus estimate h_1 from (28) (Table 1, first row). The value thus obtained is then compared to the observed value of the

TABLE 1. Semienclosed seas energy fluxes and estimated values. For the Black Sea these values are published from the literature as explained in the text.

Sea name	$V^{-1}\int_A Q_b\,dx\,dy$ (m s^{-3})	$V^{-1}\,F$ (m^2 s^{-3})	h_1 (m)	$(V\rho_0)^{-1}\int_A \boldsymbol{\tau}\cdot\mathbf{u}_s\,dx\,dy$ (m^2 s^{-3})	V (m^3)
Mediterranean	-4.36×10^{-12}	7.80×10^{-10}	179	1.12×10^{-9}	3.28×10^{15}
Black	1.04×10^{-11}	-3.11×10^{-10}	30	3.60×10^{-10}	5.47×10^{14}
Red	-2.72×10^{-11}	2.72×10^{-9}	100	1.23×10^{-10}	2.11×10^{14}
Baltic	5.87×10^{-11}	-7.04×10^{-10}	12	9.15×10^{-9}	1.89×10^{13}

interface h_1. Encouraged by the agreement of the estimate in the Mediterranean, we evaluate the energy flux of other seas by using the values of Q_b and h_1, estimated from models and observations, in (12) to evaluate the energy flux at the strait (Table 1). With this estimate, supplemented by the evaluation of the wind work from models, we are in a position to discuss the energetics of these semienclosed seas and characterize some aspects of their dynamics on the basis of the balances in (29).

a. The Mediterranean Sea

For the Mediterranean, Adani et al. (2011) have produced a 23-yr reanalysis using a high-resolution ocean model (1/16° in the horizontal, 71 levels in the vertical), and all the available in situ observations of temperature and salinity plus along-track satellite sea level anomalies for that period. The wind forcing is derived from the operational European Centre for Medium-Range Weather Forecasts (ECMWF) analyses (for the period 1993–2007), rather than the 15-yr ECMWF Re-Analysis (ERA-15) wind reanalysis (used for the period 1985–92, for which the higher-resolution product is not available) because of its higher accuracy and resolution.

The reanalysis dataset of Adani et al. (2011) allows for the evaluation of the mechanical energy flux at the strait F, as well as Q_b, $\langle b_t\rangle$ and the wind work. The energy flux at the Strait of Gibraltar is evaluated at longitude 5.4°W, close to the easternmost end of the strait, and thus downstream of the shallowest sill. At this longitude we expect the composite Froude number G to be small, and thus the approximation of (28) should be accurate. Pinardi et al. (2014) have evaluated the diffusive flux of buoyancy at the Strait of Gibraltar and found it to be four orders of magnitude smaller than the surface integral of Q_b. Thus, the term D is completely negligible in (28), and it is not included in the estimate. Figure 3 shows F and the terms composing (12) evaluated for the Mediterranean Sea. We note that F is positive, which implies that energy is entering the Mediterranean Sea from the North Atlantic Ocean through the Strait of Gibraltar. It is clear from Fig. 3 that the kinetic energy contribution (gray dotted line in Fig. 3) is negligible compared to the pressure (black dashed) and potential energy (black solid) terms (by a factor larger than 10), confirming that G^2 is indeed small.

To evaluate the terms in the surface buoyancy flux, Q_b in (8), the following values have been chosen:

$$\rho_o = 1029\,\mathrm{kg\,m^{-3}},\quad \beta_T = 2.3\times10^{-4}\,^\circ\mathrm{C}^{-1},$$
$$\beta_S = 7.5\times10^{-4}\,\mathrm{psu}^{-1},\quad C_w = 3990\,\mathrm{J\,kg^{-1}\,^\circ C^{-1}},\quad \text{and}$$
$$S_0 = 38.7\,\mathrm{psu},\tag{31}$$

where we assumed the surface salinity to be a constant with an error of a few percent with respect to the real salt flux used by the model. In Fig. 4, we show the terms on the right-hand side of (28); the surface buoyancy flux (upper panel of Fig. 4) and the time derivative of the volume-averaged buoyancy almost balance each other and the resulting difference is a high-frequency time series (lower panel of Fig. 4). The difference time series shows a multidecadal trend that could be ascribed to long-term climate variability, as shown in other papers (Pettenuzzo et al. 2010). Our time series does not resolve this multidecadal signal, and thus we compare the time mean values in the terms of (28). The time mean values of the wind work and buoyancy flux are comparable with those published in Korres et al. (2000).

In the time mean, only the surface buoyancy flux Q_b should contribute to the right-hand side of (28): considering this term only, the resulting value of h_1 is

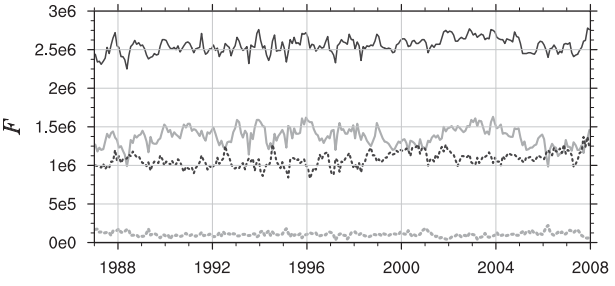

FIG. 3. The section integrals of the energy flux components (m^5 s^{-3}) of (12) for the period 1987–2008: kinetic energy $-1/2\int_{\mathrm{OB}}\int(u^2+v^2)\mathbf{u}\cdot\hat{\mathbf{n}}\,dz\,dl$ (gray dotted); pressure work $-\int_{\mathrm{OB}}\int p/\rho_o\mathbf{u}\cdot\hat{\mathbf{n}}\,dz\,dl$ (black dashed); potential energy flux $\int_{\mathrm{OB}}\int zb\mathbf{u}\cdot\hat{\mathbf{n}}\,dz\,dl$ (gray solid); and the total F (black solid).

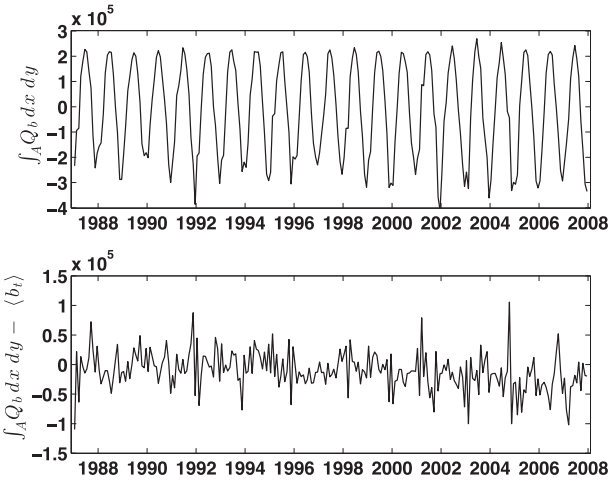

FIG. 4. The (top) surface buoyancy flux Q_b integrated over the area of the Mediterranean Sea (1987–2008) and (bottom) difference from the time derivative of the volume averaged buoyancy ($m^4 s^{-3}$).

reported in Table 1. This estimated value is within those expected for the interface depth at the Camarinal Sill of the Strait of Gibraltar, which ranges from 180 to 220 m, depending on the definition (Sánchez-Román et al. 2009). Our time series is too short for the second term on the right-hand side of (28) to be completely negligible; when it is included, h_1 becomes 234 m, that is, about 55 m different from the previous estimate. Sánchez-Román et al. (2009) found a comparable difference between estimates of the interface depending on whether the definition of h_1 is chosen as the line of zero velocity field ($h_1 = 180$ m) or as the depth of the velocity shear maximum ($h_1 = 220$ m). We thus conclude that within the uncertainty in the definition of h_1, the approximation (28) works well for the Mediterranean.

The general conclusion for the Mediterranean Sea is that both the wind work and buoyancy fluxes contribute in comparable proportion to sustain the mechanical energy of the circulation, giving rise to an antiestuarine circulation with a relatively high energy.

b. The Black, Red, and Baltic Seas

For the Black Sea, it is possible to estimate the values of Q_b, h_1, and the wind work from published work. For the Baltic and the Red Seas, Q_b and h_1 can be obtained from the published literature, but we were unable to find the wind work, so the latter was calculated using the Centro Euro-Mediterraneo sui Cambiamenti Climatici (CMCC) Global Ocean Reanalysis System (C-GLORS) at ½° resolution. The C-GLORS product is described in detail in Storto et al. (2011), and it consists of a three-dimensional global ocean variational assimilation system that uses all the available in situ observations as well as along-track sea level anomaly observations for the period 1993–2003. As in the Mediterranean, the diffusive flux through the strait is neglected.

1) THE BLACK SEA

For the Black Sea, we take the high-resolution model calculations of Rachev and Stanev (1997) as the best estimate, where the rate of the wind work per unit mass is reported to be $3.6 \times 10^{-10}\,m^2\,s^{-3}$.

The values of the annual and basin average heat and freshwater fluxes vary substantially depending on the model: according to Stanev et al. (2003, p. 68), the annual and basin average is $Q_b = 3.3 \times 10^{-9}\,m^2\,s^{-3}$; according to Kara et al. (2008, their Fig. 6), the annual and basin average is $Q_b = 1.3 \times 10^{-8}\,m^2\,s^{-3}$ [the sign convention for the fluxes in Stanev et al. (2003) and Kara et al. (2008) is opposite ours]. The two estimates differ by a factor of 3, and this discrepancy is indicative of large uncertainties attributable to model dependences on parameters and resolution. In Table 1 we report the most recent estimate, $Q_b = 1.3 \times 10^{-8}\,m^2\,s^{-3}$ (Kara et al. 2008). This value needs to be multiplied by the surface area ($4.36 \times 10^{11}\,m^2$) and divided by the volume in Table 1.

To evaluate F, we need an estimate of the upper-layer depth at the strait, which we derive from the observations of Gregg and Özsoy (2002) at the mouth of the Bosphorus Strait (cf. their Fig. 3b). This estimate of h_1 together with the integral of Q_b leads to a value of F that is very close in absolute value to the rate of the wind work (all reported in the second row in Table 1). The contribution of F is negative in (29), and thus F opposes the wind work, leading to a small positive net energy source resulting from the combination of wind and buoyancy forcings. It is thus not surprising that the currents in the Black Sea are confined to a very shallow region and that the general level of energy is low. The energy flux at the strait is such as to extract energy from the basins, and the rate of the wind work barely overcomes this energy sink.

2) THE RED SEA

For the Red Sea we have been unable to find published estimates of the rate of the wind work, and we evaluated this quantity using the C-GLORS dataset. The time series of the rate of wind work per unit area is shown in Fig. 5 (middle) and should be compared to those for the Mediterranean (top) and the Baltic (bottom). The most striking characteristic of the Red Sea time series is the negative rate of the wind work that appears at the beginning of each year, coincident with the reversed wind stress that occurs in the southern part of the basin in late winter and associated with the winter Indian monsoon. This reversal is responsible for the low

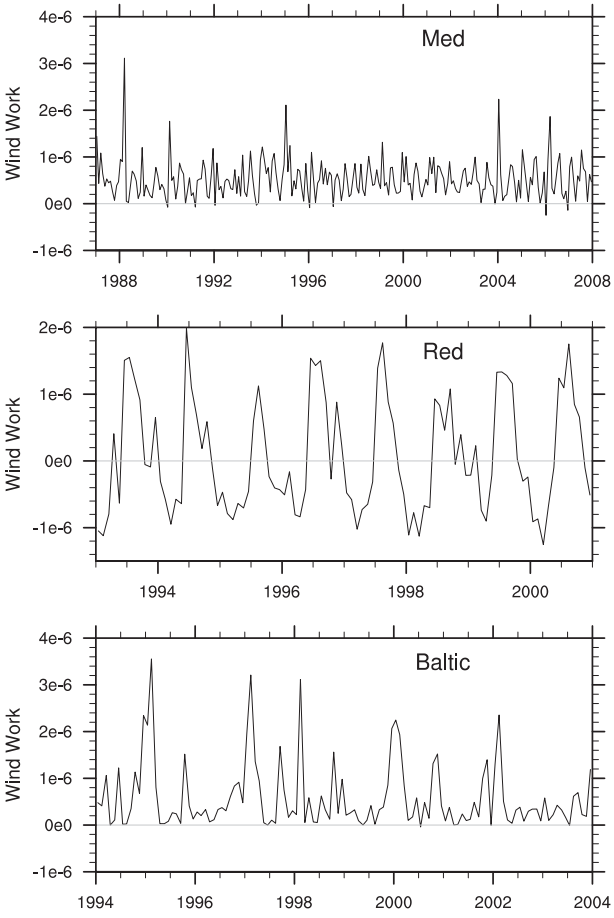

FIG. 5. The rate of the wind work per unit area ($m^3 s^{-3}$) for the (top) Mediterranean Sea, (middle) Red Sea, and (bottom) Baltic Sea.

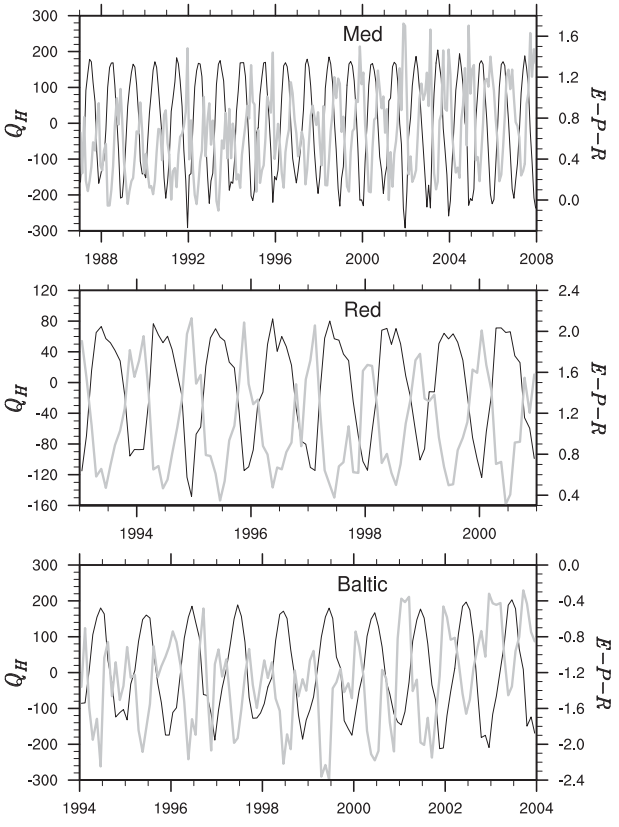

FIG. 6. The heat flux Q_H (thin black lines) and $E - P - R$ (thick gray line), both averaged over the surface of each basin, for the (top) Mediterranean Sea, (middle) Red Sea, and (bottom) Baltic Sea. The units of (left) Q_H are watts per square meter and those of (right) $E - P - R$ are meters per year.

values of the time-averaged rate of the wind work, reported in Table 1 (third row in Table 1). It is probable that higher-resolution calculations would increase the correlation between the surface currents and the wind stress, leading to a larger estimate of the rate of the wind work. Indeed, experience with the assimilation in the Mediterranean indicates that high resolution in models and accuracy in wind forcing fields are necessary to obtain a satisfactory reanalysis.

Using the same dataset, we have also evaluated the surface heat and freshwater fluxes (see Fig. 6). To obtain the corresponding buoyancy flux, we used the same parameters (31) of the Mediterranean Sea except for the surface salinity, which is $S_0 = 39$ psu. The values obtained from the C-GLORS are smaller by about a factor of 2 than the estimates of Sofianos et al. (2002). However, changing these values by two would not change our interpretation of the energy balance in this basin.

The estimates of h_1 derive from the velocity zero crossings at Bab el Mandeb reported by Sofianos et al. (2002). As shown in that work, the velocity at Bab el Mandeb can be approximated with a two-layer exchange for most of the year, except for four summer months (June–September) when a third layer becomes apparent. In spite of this complication, Sofianos et al. (2002) show that the depth of the interface between the top and bottom layers is, on average, about 100 m.

From our analysis, the energetics of the Red Sea are qualitatively similar to the Mediterranean case, in that buoyancy and wind result in an energy source (cf. the first and third rows in Table 1). An important quantitative difference is the dominance of the ''buoyancy'' component over the wind forcing in the Red Sea, in accordance with the modeling results of Sofianos and Johns (2003).

3) THE BALTIC SEA

For the Baltic, we have calculated the rate of the wind work, heat flux, and freshwater flux using the C-GLORS assimilation system at ½°, averaged over the years 1994–2003. The rate of wind work per unit area is shown in Fig. 5 (bottom) and has a higher amplitude than both the

Mediterranean Sea (top) and the Red Sea (middle). The time and basin averages of the heat and freshwater fluxes in the C-GLORS assimilation are $-2.3\,\mathrm{W\,m^{-2}}$ for Q_H and $-1.2\,\mathrm{m\,yr^{-1}}$ for $E - P - R$ (see Fig. 6). These values are in the range found with observations and regional models for the Baltic Sea [cf. Tables 1 and 2 of Meier and Doscher (2002)]. To convert the heat and freshwater flux into a buoyancy flux, we use the values in (31), except that the surface salinity is $S_0 = 6$ psu. The estimate of h_1 derives from the analyses of Jakobsen and Trébuchet (2000) and She et al. (2007), showing that the depth of the interface between the outflowing fresh layer and the inflowing saltier layer at the Danish Straits (Fehmarn Belt and Great Belt) is at 13 and 10 m, respectively. Finally, the value of F is estimated in Table 1 (third row). The very low value of surface salinity, combined with the shallow depth of the Danish Straits, drives down the estimate of the energy flux due to buoyancy.

As in the Black Sea, the energy flux at the strait is a sink of energy, opposing the rate of the wind work. However, in the Baltic Sea the rate of the wind work is one order of magnitude larger than the energy flux at the strait, indicating that the circulation per unit volume should be more energetic than that of the Black Sea (cf. the second and fourth rows in Table 1).

5. Conclusions

In this paper, we have deduced and discussed the consistent mechanical energy budget for semienclosed seas with vertically separated exchange flow at the strait. Under these conditions, the flux of potential energy and pressure work through the strait can be related, in steady state, to the net surface buoyancy flux. The time rate of change of the volume-integrated mechanical energy of the semienclosed basins is then directly related to the rate of the wind work, surface heat, and freshwater fluxes. This is in contrast to the energy budget of closed ocean basins where the net freshwater and heat surface fluxes must integrate to zero in steady state, and the global energy is driven by the mechanical work due to the wind (and tides).

The energetics analysis of semienclosed seas allows some insight into the differences between estuarine and antiestuarine circulations and also among the same kind of semienclosed circulations. It is found that the energy flux at the strait can be either a source or sink of energy, depending on the sign of the net surface buoyancy flux, negative or positive, respectively, and it can oppose or reinforce the wind work.

We have analyzed the four major semienclosed seas with exchange flows in the World Ocean: the Mediterranean and Red Seas are examples of antiestuarine dynamics, and the Black and Baltic Seas are estuarine counterparts. In the case of the Mediterranean Sea, the theory was confirmed by calculating the energy terms from a high-resolution reanalysis dataset that allows for the estimation of the proportionality constant between lateral energy fluxes at the strait and the net surface buoyancy flux. The methodology was then generalized to the other basins, where a long and consistent dataset of ocean reanalyses is not available.

The results indicate that the main difference in the energy balance of the estuarine and antiestuarine basins is the energy sink/source role of the buoyancy flux. For the estuarine cases, the Black and Baltic Seas, the buoyancy flux is a sink of energy that counterbalances the positive wind work energy input. For the Black Sea in particular, the buoyancy flux energy term almost completely balances the rate of the wind work, thus giving rise to a low kinetic energy basin circulation. This result is consistent with the observed stagnant circulation below the strait sill depth. Instead, in the Baltic Sea the wind work largely exceeds the loss of energy from the buoyancy flux at the strait, allowing for a much higher level of kinetic energy and a substantial circulation below the sill depth.

On the antiestuarine side, the Mediterranean and Red Seas, the wind and buoyancy effects both provide an energy source for the circulation. However, these two basins differ quantitatively in that the buoyancy and wind components of the energy source are comparable in the Mediterranean, while in the Red Sea the rate of the wind work is much smaller than the buoyancy work. We recognize that the reanalysis products used for the Red and Baltic Seas are probably inadequate to estimate the rate of the wind work, and subsequent analyses will likely revise these values upward. Nevertheless, our preliminary assessment confirms the notion that buoyancy, rather than wind stress, is the essential mechanism powering the basin-scale circulation of the Red Sea, while the rate of the wind work is as important as the buoyancy to power the Mediterranean Sea.

The energy budgets so formulated are consistent with Knudsen's relation in explaining the fundamental difference in circulation dynamics of adjacent seas with a two-layer exchange flow at the strait. Freshwater and energy conservation are only two constraints arising from the pointwise equation of motion and thermodynamics, from which the details of the circulation are determined, but they appear to determine qualitative aspects of the circulation in semienclosed seas.

In our analysis we have not considered semienclosed seas with multiple strait connections to the ocean (type B in Fig. 1). In these basin types, a substantial barotropic

component of the velocity at each entry point can accompany the baroclinic flow. A barotropic flow at the strait correlates with a depth-independent pressure to give an important contribution to F. Such a term is not obviously connected to the surface buoyancy flux and does not lend itself to a simple relation with other globally constrained quantities.

Acknowledgments. We are very grateful to Andrea Storto and Simona Masina for providing the C-GLORS datasets for the Red and Baltic Seas. The anonymous referees are gratefully acknowledged for their insightful and constructive reviews. PC is supported by the Office of Science (BER), U.S. Department of Energy, Grant DE-SC0005100, and NSF Grant OCE-1258887; NP is supported by Project NextData given to INGV, Bologna Section; and LL is supported by the GEMINA Project to CMCC.

APPENDIX A

Nonlinear Equation of State

In this appendix the results of section 2 are generalized to the case of a nonlinear EOS. As an example, we use the approximation to the EOS given by de Szoeke (2004), where the specific volume is given by

$$\frac{1}{\rho}=\frac{1}{\rho_o}\left[1+\frac{g\hat{z}}{c^2}+\beta_T\theta(1-\gamma g\hat{z})+\frac{\beta_T^*}{2}\theta^2-\beta_s(S-S_o)\right], \tag{A1}$$

where $\hat{z}\equiv z-z_o$ is the depth referenced to the level z_o. Given this EOS and following Young (2010), we define the buoyancy b as

$$\frac{1}{\rho}\equiv\frac{1+b/g}{\rho_o}, \tag{A2}$$

so that

$$b=g\left[\frac{g\hat{z}}{c^2}+\beta_T\theta(1-\gamma g\hat{z})+\frac{\beta_T^*}{2}\theta^2-\beta_s(S-S_o)\right]. \tag{A3}$$

Given this definition, Young (2010) defines the potential energy $\tilde{h}^\dagger$ as

$$\tilde{h}^\dagger\equiv\int_z^0 b(\theta,S,z')\,dz', \tag{A4}$$

where the integral is performed at fixed θ and S. Thus, given the EOS, the potential energy has the form (setting $z_o=0$)

$$\tilde{h}^\dagger=g\left[-\frac{g}{2c^2}z^2-\beta_T\theta(z-\gamma g z^2)+\frac{\beta_T^*}{2}\theta^2 z-\beta_s(S-S_o)z\right]. \tag{A5}$$

The equation for energy conservation analogous to (11) is then

$$\partial_t\left\langle\frac{u^2+v^2}{2}+\tilde{h}^\dagger\right\rangle=\tilde{F}+\int_A\frac{\boldsymbol{\tau}\cdot\mathbf{u}_s}{\rho_o}dx\,dy+\langle\dot{\theta}\tilde{h}_\theta^\dagger+\dot{S}\tilde{h}_S^\dagger\rangle-\langle\nu(|\nabla u|^2+|\nabla v|^2)\rangle-\langle\nu_v(u_z^2+v_z^2)\rangle$$
$$-\int_{\mathrm{OB}}\int\nu\frac{\nabla(u^2+v^2)}{2}\cdot\hat{\mathbf{n}}\,dz\,dl, \tag{A6}$$

and where we have made the definition

$$\tilde{F}\equiv-\int_{\mathrm{OB}}\int\left(\frac{u^2+v^2}{2}+\frac{p}{\rho_o}+\tilde{h}^\dagger\right)\mathbf{u}\cdot\hat{\mathbf{n}}\,dz\,dl, \tag{A7}$$

where $\dot{\theta}$ and $\dot{S}$ are the sources of temperature and salinity, respectively. We write them as (neglecting horizontal diffusion terms)

$$\dot{\theta}=(\kappa_\theta\theta_z)_z\quad\text{and}\quad\dot{S}=(\kappa_S S_z)_z. \tag{A8}$$

Thus, the thermodynamical forcing terms appearing in the energy equation are

$$\langle\dot{\theta}\tilde{h}_\theta^\dagger+\dot{S}\tilde{h}_S^\dagger\rangle=\langle\kappa_\theta\theta_z[\beta_T(1-\gamma g z)-\beta_T^*(\theta z)_z]-\kappa_S S_z\beta_s\rangle. \tag{A9}$$

As in the linear EOS case, the surface thermodynamic forcing does not appear in the energy equation, and only the small volume terms proportional to diapycnal processes appear.

The relation between the energy flux at the open boundary $\tilde{F}$ and the surface temperature and salinity forcing is revealed by examining the θ and S equation. Here, we make the approximation that at the strait we can neglect the nonlinear terms in the EOS. This is an excellent approximation as long as the strait is shallow. Specifically, we approximate $\tilde{F}$ with

$$\tilde{F} \approx -\int_{\mathrm{OB}} \int \left[\int_0^z (\beta_T \theta - \beta_S S)\, dz' - (\beta_T \theta - \beta_S S) z \right] \mathbf{u} \cdot \hat{\mathbf{n}}\, dz\, dl\,. \tag{A10}$$

In this case, in order to relate $\tilde{F}$ to the thermodynamical forcing, we need to consider the linear combination of the θ and S equations, rather than the buoyancy equation, and the results of sections 2 and 3 are recovered with the following modification:

$$\tilde{F} \approx -h_1 \left(\int_A Q_b\, dx\, dy - \partial_t \langle \beta_T \theta - \beta_S S \rangle \right). \tag{A11}$$

APPENDIX B

Knudsen Relations

In this section we derive Knudsen relations in the context of the rigid lid approximation, where the mass flux due to $E - P - R$ is neglected in the mass conservation equation, but is included in the salinity surface boundary condition. This derivation leads to essentially the same result as Knudsen's original formulation, and it is shown here for consistency with our treatment throughout the paper.

Considering a two-layer exchange flow at the strait, the mass budget over a semienclosed basin in the rigid lid approximation requires

$$T_1 + T_2 = 0, \tag{B1}$$

where T_1 (T_2) refers to the upper-layer (lower layer) transport at the strait, positive into the semienclosed basin. The transport is computed over the arclength of the strait. Unlike the original Knudsen's treatment, the mass input (or loss) attributable to the net $E - P - R$ is neglected.

The $E - P - R$ enters as a salt flux in the salinity budget, which, in steady state, requires

$$T_1 S_1 + T_2 S_2 = \int_A S_0 (E - P - R)\, dx\, dy, \tag{B2}$$

where S_1 (S_2) denotes the upper-layer (lower layer) salinity at the strait, assumed to be approximately constant along the strait arclength, and S_0 is the surface salinity.

Using the mass and salt conservation, one obtains the following relations for the volume transports:

$$T_1 = \frac{\int_A S_0 (E - P - R)\, dx\, dy}{S_2 - S_1} \quad \text{and} \tag{B3}$$

$$T_2 = -\frac{\int_A S_0 (E - P - R)\, dx\, dy}{S_2 - S_1}. \tag{B4}$$

Because $S_2 > S_1$ for positive salt stratification, a positive net $E - P - R$ leads to upper-layer inflow into the semienclosed sea and negative lower-layer outflow.

In our notation, the original Knudsen treatment would read

$$T_1 = S_2 \frac{\int_A (E - P - R)\, dx\, dy}{S_2 - S_1} \quad \text{and} \tag{B5}$$

$$T_2 = -S_1 \frac{\int_A (E - P - R)\, dx\, dy}{S_2 - S_1}, \tag{B6}$$

and they differ from (B3) and (B4) by a term of order $(S_2 - S_1)/S_0$, which is small in the Boussinesq approximation.

REFERENCES

Adani, M., S. Dobricic, and N. Pinardi, 2011: Quality assessment of a 1985–2007 Mediterranean Sea reanalysis. *J. Atmos. Oceanic Technol.,* **28,** 569–589.

Cuypers, Y., P. Bouruet-Aubertot, C. Marec, and J.-L. Fuda, 2012: Characterization of turbulence from a fine-scale parameterization and microstructure measurements in the Mediterranean Sea during the BOUM experiment. *Biogeosciences,* **9,** 3131–3149.

de Szoeke, R. A., 2004: An effect of the thermobaric nonlinearity of the equation of state: A mechanism for sustaining solitary Rossby waves. *J. Phys. Oceanogr.,* **34,** 2042–2056.

Gayen, B., R. W. Griffiths, G. O. Hughes, and J. A. Saenz, 2013: Energetics of horizontal convection. *J. Fluid Mech.,* **716,** R10, doi:10.1017/jfm.2012.592.

Gregg, M. C., and E. Özsoy, 1999: Mixing on the Black Sea shelf north of the Bosphorus. *Geophys. Res. Lett.,* **26,** 1869–1872.

——, and ——, 2002: Flow, water mass changes, and hydraulics in the Bosphorus. *J. Geophys. Res.,* **107** (C3), doi:10.1029/2000JC000485.

Jakobsen, F., and C. Trébuchet, 2000: Observations of the transport through the Belt Sea and an investigation of the momentum balance. *Cont. Shelf Res.,* **20,** 293–311.

Kara, A. B., A. J. Wallcraft, H. E. Hurlburt, and E. Stanev, 2008: Air–sea fluxes and river discharges in the Black Sea with a focus on the Danube and Bosphorus. *J. Mar. Syst.,* **74,** 74–95.

Knudsen, M., 1900: Ein hydrographischer lehrsatz. *Ann. Hydrogr. Marit. Meteor.,* **28,** 316–320.

Korres, G., N. Pinardi, and A. Lascaratos, 2000: The ocean response to low-frequency interannual atmospheric variability in the Mediterranean Sea. Part I: Sensitivity experiments and energy analysis. *J. Climate,* **13,** 705–731.

Meier, H. M., and R. Doscher, 2002: Simulated water and heat cycles of the Baltic Sea using a 3D coupled atmosphere–ice–ocean model. *Boreal Environ. Res.,* **7,** 327–334.

Murray, S. P., and W. Johns, 1997: Direct observations of seasonal exchange through the Bab el Mandab Strait. *Geophys. Res. Lett.,* **24,** 2557–2560.

Osborn, T., 1980: Estimates of the local rate of vertical diffusion from dissipation measurements. *J. Phys. Oceanogr.,* **10,** 83–89.

Paparella, F., and W. R. Young, 2002: Horizontal convection is non-turbulent. *J. Fluid Mech.,* **466,** 205–214.

Pettenuzzo, D., W. G. Large, and N. Pinardi, 2010: On the corrections of ERA-40 surface flux products consistent with the Mediterranean heat and water budgets and the connection between basin surface total heat flux and NAO. *J. Geophys. Res.,* **115,** C06022, doi:10.1029/2009JC005631.

Pickard, G., and W. Emery, 1982: *Descriptive Physical Oceanography: An Introduction.* 4th ed. Pergamon Press, 265 pp.

Pinardi, N., A. Bonaduce, A. Navarra, S. Dobricic, and P. Oddo, 2014: The mean sea level equation and its application to the Mediterranean Sea. *J. Climate,* **27,** 442–447.

Pratt, L. J., and J. A. Whitehead, 2008: *Nonlinear Topographic Effects in the Ocean and Atmosphere.* Springer, 589 pp.

Rachev, N. H., and E. V. Stanev, 1997: Eddy processes in semi-enclosed seas: A case study for the Black Sea. *J. Phys. Oceanogr.,* **27,** 1581–1601.

Sánchez-Román, A., G. Sannino, J. García-Lafuente, A. Carillo, and F. Criado-Aldeanueva, 2009: Transport estimates at the western section of the Strait of Gibraltar: A combined experimental and numerical modeling study. *J. Geophys. Res.,* **114,** C06002, doi:10.1029/2008JC005023.

Sannino, G., A. Bargagli, and V. Artale, 2002: Numerical modeling of the mean exchange through the Strait of Gibraltar. *J. Geophys. Res.,* **107** (C8), doi:10.1029/2001JC000929.

She, J., P. Berg, and J. Berg, 2007: Bathymetry impacts on water exchange modelling through the Danish Straits. *J. Mar. Syst.,* **65,** 450–459.

Sofianos, S. S., and W. E. Johns, 2003: An oceanic general circulation model (OGCM) investigation of the Red Sea circulation: 2. Three-dimensional circulation in the Red Sea. *J. Geophys. Res.,* **108,** 3066, doi:10.1029/2001JC001185.

——, ——, and S. Murray, 2002: Heat and freshwater budgets in the Red Sea from direct observations at Bab el Mandeb. *Deep-Sea Res. II,* **49,** 1323–1340.

Spall, M. A., 2003: On the thermohaline circulation in flat bottom marginal seas. *J. Mar. Res.,* **61,** 1–25.

Stanev, E., M. J. Bowman, E. L. Peneva, and J. V. Staneva, 2003: Control of Black Sea intermediate water mass formation by dynamics and topography: Comparison of numerical simulations, surveys and satellite data. *J. Mar. Res.,* **61,** 59–99.

Storto, A., S. Dobricic, S. Masina, and P. Di Pietro, 2011: Assimilating along-track altimetric observations through local hydrostatic adjustment in a global ocean variational assimilation system. *Mon. Wea. Rev.,* **139,** 738–754.

Tsimplis, M., R. Proctor, and R. Flather, 1995: A two-dimensional tidal model for the Mediterranean Sea. *J. Geophys. Res.,* **100** (C8), 16 223–16 239.

Winters, K. B., and W. R. Young, 2009: Available potential energy and buoyancy variance in horizontal convection. *J. Fluid Mech.,* **629,** 221–230.

Wunsch, C., and R. Ferrari, 2004: Vertical mixing, energy, and the general circulation of the oceans. *Annu. Rev. Fluid Mech.,* **36,** 281–314.

Young, W. R., 2010: Dynamic enthalpy, conservative temperature, and the seawater Boussinesq approximation. *J. Phys. Oceanogr.,* **40,** 394–400.